ACS Sustainable Chemistry & Engineering

Research Article

pubs.acs.org/journal/ascecg

Organic Sensitizers Featuring 9,10-Diaryl-Substituted Anthracene Unit

Huiyang Li,[†] Yizhou Yang,[†] Yingqin Hou,[†] Runli Tang,[†] Tainan Duan,[†] Junnian Chen,[†] Heng Wang,[‡] Hongwei Han,[‡] Tianyou Peng,[†] Xingguo Chen,[†] Qianqian Li,*[,†] and Zhen Li[†]

[†]Department of Chemistry, Hubei Key Lab on Organic and Polymeric Optoelectronic Materials, Wuhan University, Wuhan 430072, China

[‡]Michael Grätzel Center for Mesoscopic Solar Cells, Wuhan National Laboratory for Optoelectronics, Huazhong University of Science and Technology, Wuhan 430072, China

Supporting Information

ABSTRACT: A series of anthracene-based dyes were designed and employed in dye-sensitized solar cells in which different 9,10-diaryl-substituted anthracene groups acted as a π-bridge with 2,6-linkage mode. The *tert*-butylphenyl and hexyloxyphenyl groups in the 9 and 10 positions of the anthracene unit were almost perpendicular to the conjugated plane, which would be beneficial to suppressing the possible $\pi-\pi$ stacking and retarding the charge recombination. Their photophysical properties and photovoltaic performance could be tuned by the modification of the substituted groups to the anthracene ring in some degree. Consequently, dye **LI-59**-based solar cells gave the best performance, with a J_{sc} (short circuit current) of 13.42 mA cm^{-2}, V_{oc} (open circuit voltage) of 722 mV, and FF (fill factor) of 0.66, corresponding to an overall conversion efficiency of 6.42% without the presence of CDCA.

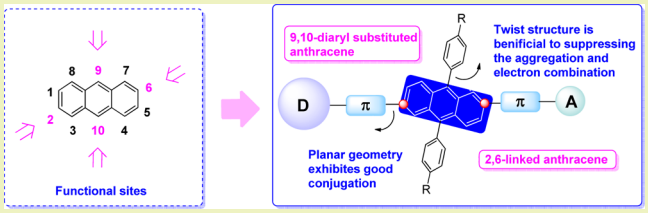

KEYWORDS: *9,10-Diaryl-substituted anthracene, $\pi-\pi$ Stacking, Organic sensitizer, Intramolecular charge transfer, Dye-sensitized solar cell*

INTRODUCTION

Dye-sensitized solar cells (DSCs) have been extensively studied due to their high performance in converting solar energy to electricity at a relatively low cost.[1−4] In DSCs, the photosensitizer is the key component for light harvesting and electron injection. In addition to the metal-based sensitizers,[5−9] the metal-free organic sensitizers attracted great attention for their relatively cost-effective facile preparation processes, convenient structural modification, and high molar extinction coefficients.[10−14] For the donor−π−acceptor (D−π−A) structure in most metal-free organic sensitizers, the variation of the π-bridge has led to huge array of dyes, displaying promising energy conversion efficiencies and intense incident photon-to-current efficiencies (IPCE).[15−19] Especially, the utilization of many fused aromatic rings with big and planar π-conjugations[20−23] could benefit to the charge transfer and light harvesting. However, unfortunately, the planar configuration usually caused strong intermolecular interactions, resulting in a decrease in conversion efficiency. Thus, many efforts have been attempted to tackle this problem.[24−26]

Anthracene, which possessed a good planar structure, could be modified at four different points (Chart 1), making its functionalization more convenient and flexible.[27−29] Actually, anthracene derivatives have been successfully developed for applications in light-emitting diodes,[30−33] thin film transistors,[34,35] and even bulk heterojunction solar cells.[36,37] However, reports of their utilization in DSCs are still scarce.[38,39] To introduce the anthracene block into the donor−π−acceptor dyes as a π-bridge, in principle, there are two approaches: one is through the C9 and C10 positions, while another is through the C2 and C6 positions. Once linked through its C9 and C10 sites,[40] the whole molecule, as a result of the steric effect caused by the four hydrogen atoms at the C1, C2, C5 and C8 sites, would be twisted at the connecting positions of the anthracene and other aromatic rings, thus, hampering the effective intramolecular charge transfer (ICT) and being harmful to the performance of the corresponding DSCs.[41] In contrast to this, the 2,6-linkage mode could keep relatively good planar configuration of the whole conjugated system and broaden its absorption spectrum, leading to good performance.[42−46] However, once again, good planar structure usually caused unwanted $\pi-\pi$ stacking, resulting in possibly decreased performance. Thus, if these $\pi-\pi$ interactions could be avoided to some degree, the energy conversion efficiencies might be improved, as partially confirmed by some related papers published recently.[47−49] For example, once incorporating the 2,6-conjugated 9,10-bishexyloxyanthracene unit as the conjugated bridge, the sensitizers gave conversion efficiencies in the

Received: January 13, 2014
Revised: May 14, 2014
Published: May 20, 2014

Chart 1. Structure of Anthracene-Based Dyes LI-58-LI-61 and Reference Dyes

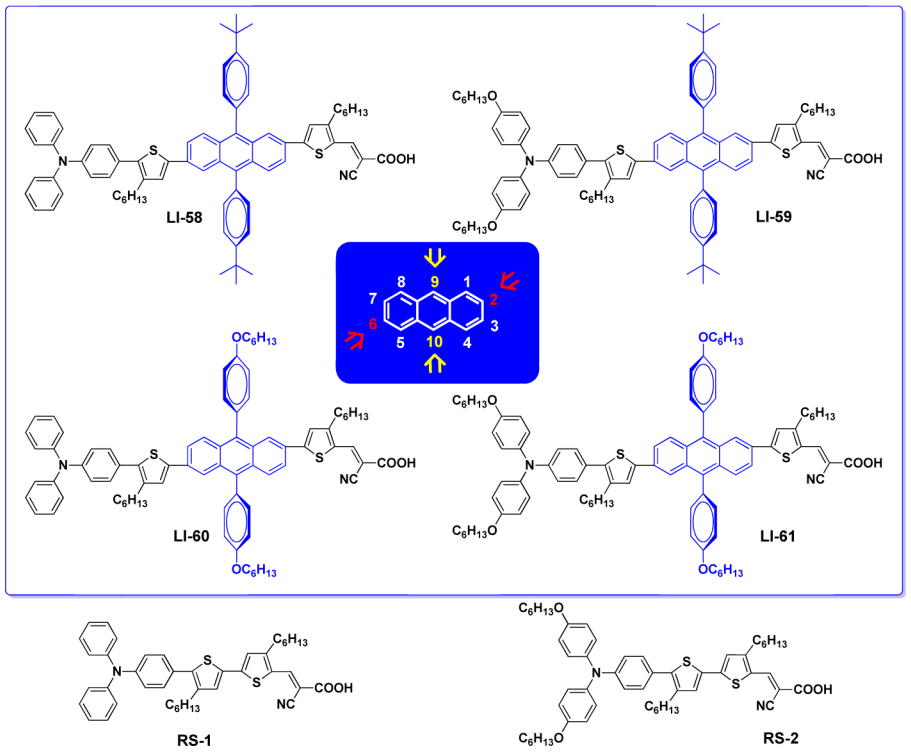

range of 4.69−7.52%.[42] While through suitable modification of the anthrancene unit, high quality films of the corresponding dyes could be formed on the TiO_2 surface to improve the performance.[39]

Considering the two above linkage modes carefully, perhaps the four functional sites of the anthracene ring could be intelligently utilized. To realize good planar configuration of the dyes with D−π−*A* structure, the anthracene moieties can be incorporated as the conjugated bridge through the 2,6-linkage mode. At the same time, some aromatic groups could be substituted to the C9 and C10 positions, which could act as the isolation groups to suppress the harmful π−π stacking and dye aggregations. Also, there are large dihedral angles between the anthracene unit and substitutes at 9,10-positions, thus, the presence of these substitutes would not affect the π-conjugation of the whole molecule. Furthermore, some alkoxy or alkyl chains can be easily introduced to the 9,10-substituted aromatic rings, to improve the solubility of dyes and inhibit the unexpected electron recombination (Chart 1). From this idea, a series of organic dye sensitizers bearing 9,10-diaryl-substituted and 2,6-linked anthracene units as the conjugated bridge were designed and prepared, in which triphenylamine or its derivative acted as the donor and cyanoacetic acid as the acceptor and anchoring group. In addition, thiophene rings were incorporated into the bridge to further expand the absorption spectra and improve the solubility, and 4-*tert*-butylphenyl or 4-hexyloxyphenyl groups were linked to the 9 and 10 positions of the anthracene as the isolation groups to suppress dye aggregation and electron recombination. Fortunately, these sensitizers demonstrated relatively high conversion efficiencies. Moreover, in order to highlight the function of the anthracene moieties, two reference sensitizers (Chart 1, **RS-1**[50] and **RS-2**) were synthesized for comparison. Herein, we report their syntheses, structural characterization, electrochemical properties, theoretical calculations, and photovoltaic performance.

EXPERIMENTAL SECTION

Materials. Tetrahydrofuran (THF) was predried over potassium hydroxide and then distilled from K−Na alloy under an atmosphere of dry argon. *N, N*-Dimethylformamide (DMF) was dried over CaH_2 and distilled under a reduced pressure. *N,N*-Diphenyl-4-(4,4,5,5- tetramethyl-1,3,2-dioxaborolan-2-yl) aniline (**TPA-B**) and 4,4,5,5-tetramethyl-2-{4-[*N,N*-bis (4-hexyloxyphenyl)amino]phenyl}-1,3,2 dioxaborolane (**OHexylTPA-B**) were prepared following the similar procedures of the literature.[51] All other reagents were used as received.

Instrumentation. ^{1}H and ^{13}C NMR spectroscopy study was performed on a Varian Mercury 300 spectrometer. MS (EI) spectra were recorded with a ZAB 3F-HF mass spectrophotometer. High resolution mass spectra (HRMS) were recorded with a Waters ESI mass spectrometer. Absorption spectra of the dyes were measured with a Shimadzu UV-2550 spectrometer. Electrochemical cyclic voltammetry was performed on a CHI 660 voltammetric analyzer using a three-electrode electrochemical cell in a solution of tetrabutylammonium hexafluorophosphate (0.1 M in anhydrous argon-purged CH_2Cl_2) with a scanning rate of 100 mV/s at room temperature. Elemental analyses were performed on a 73 CARLOERBA-1106 microelemental analyzer.

Synthesis. The synthesis of the intermediates for dyes is presented in the Supporting Information.

*Synthesis of **LI-58**.* A mixture of **6** (170 mg, 0.16 mmol) and cyanoacetic acid (42 mg, 0.49 mmol) were dissolved in the mixed solvent of MeCN (10 mL) and THF (5 mL), and then piperidine (10 μL) was added. The solution was refluxed overnight. After cooling to room temperature, the mixture was poured into a 0.1 M HCl solution (100 mL). The crude product was extracted with chloroform, washed with water, and dried over anhydrous sodium sulfate. After the solvent was evaporated under reduced pressure, the crude product was purified by column chromatography (chloroform/methanol from 100/1 to 20/1) as a dark red solid (120 mg, 66.3%). ^{1}H NMR (DMSO-d_6/$CDCl_3$ = 1/1, 300 MHz) δ (ppm): 8.27 (s, 1H, =CH−), 8.15 (s, 1H, ArH), 7.90 (s, 1H, ArH), 7.73−7.71 (m, 2H, ArH), 7.67−7.62 (m, 6H, ArH), 7.35−7.23 (m, 11H, ArH), 7.16 (s, 1H, ArH), 7.08−6.99 (m,

dx.doi.org/10.1021/sc500234a | *ACS Sustainable Chem. Eng.* 2014, 2, 1776−1784

Scheme 1. (i) *n*-BuLi, $BrC_6H_4R^2$, THF; (ii) $NaH_2PO_2{\cdot}H_2O$, KI, CH_3COOH; (iii) Tributyl(4-hexylthiophen-2-yl)stannane, $Pd(PPh_3)_4$, Toluene; (iv) DMF, $POCl_3$, $ClCH_2CH_2Cl$; (v) *N*-Bromosuccinimide; (vi) TPA-B or OHexylTPA-B, $Pd(PPh_3)_4$, THF/H_2O; and (vii) Cyanoacetic Acid, THF/CH_3CN

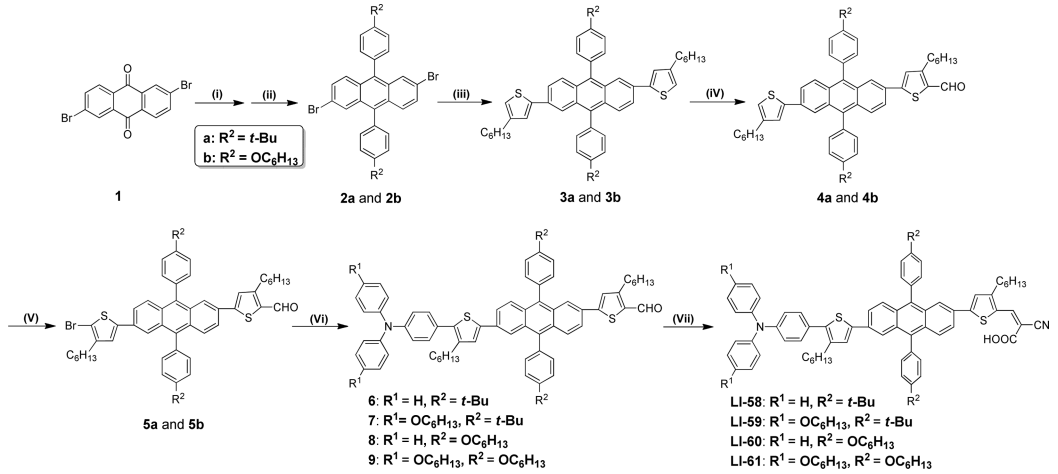

8H, ArH), 2.77 (s, br, 2H, $-CH_2-$), 2.61 (t, J = 7.8 Hz, 2H, $-CH_2-$), 1.58 (s, br, 4H, $-CH_2-$), 1.47 (s, 18H, $-CH_3$), 1.30−1.25 (m, 12H, $-CH_2-$), 0.87−0.85 (m, 6H, $-CH_3$). HRMS (ESI, m/z): $[M-1]^-$ calcd for $C_{76}H_{75}N_2O_2S_2$: 1111.5270. Found: 1111.5262. Anal. calcd for $C_{76}H_{76}N_2O_2S_2$: C, 81.97; H, 6.88; N, 2.52. Found: C, 82.08; H, 6.50; N, 2.66.

Synthesis of ***LI-59***. **LI-59** was synthesized by the similar procedure as **LI-58** described above as a dark red solid (70 mg, 78.2%). ^{1}H NMR ($CDCl_3$, 300 MHz) δ (ppm): 8.35 (s, 1H, =CH−), 8.04 (s, 1H, ArH), 7.86−7.75 (m, 3H, ArH), 7.69−7.55 (m, 6H, ArH), 7.46−7.41 (m, 4H, ArH), 7.15−7.07 (m, 8H, ArH), 7.00−6.82 (m, 6H, ArH), 3.93 (s, br, 4H, $-OCHH_2-$), 2.77 (s, br, 2H, $-CH_2-$), 2.59 (s, br, 2H, $-CH_2-$), 1.80−1.74 (m, 4H, $-CH_2-$), 1.59 (s, br, 4H, $-CH_2-$), 1.51−1.50 (m, 22H, $-CH_2-$ and $-CH_3$), 1.34−1.26 (m, 20H, $-CH_2-$), 0.91−0.87 (m, 12H, $-CH_3$). ^{13}C NMR (DMSO-d_6/$CDCl_3$ = 4/1, 75 MHz) δ (ppm): 164.7, 155.3, 155.2, 152.1, 150.5, 147.8, 143.1, 140.5, 139.9, 138.7, 138.2, 137.8, 136.8, 134.6, 134.4, 131.0, 130.6, 129.8, 129.6, 129.4, 129.3, 129.1, 128.5, 128.0, 127.6, 126.6, 126.0, 125.6, 125.4, 125.1, 124.6, 123.8, 122.7, 121.8, 119.1, 116.3, 114.9, 67.8, 34.5, 31.2, 30.8, 30.6, 29.0, 28.8, 28.7, 28.6, 25.4, 22.3, 13.8. HRMS (ESI, m/z): $[M-1]^-$ calcd for $C_{88}H_{99}N_2O_4S_2$: 1311.7046. Found: 1311.7045. Anal. calcd for $C_{88}H_{100}N_2O_4S_2$: C, 80.44; H, 7.67; N, 2.13. Found: C, 80.29; H, 7.33; N, 2.31.

Synthesis of ***LI-60***. **LI-60** was synthesized by the similar procedure as **LI-58** described above as a dark red solid (50 mg, 41.4%). ^{1}H NMR ($CDCl_3$, 300 MHz) δ (ppm): 8.39 (s, 1H, =CH), 8.10 (s, 1H, ArH), 7.92 (s, 1H, ArH), 7.76−7.71 (m, 2H, ArH), 7.63−7.54 (m, 2H, ArH), 7.40−7.37 (m, 4H, ArH), 7.26−7.16 (m, 14H, ArH), 7.06−7.04 (m, 6H, ArH), 4.14 (s, br, 4H, $-OCHH_2-$), 2.80 (s, br, 2H, $-CH_2-$), 2.63 (s, br, 2H, $-CH_2-$), 1.91 (s, br, 4H, $-CH_2-$), 1.59 (s, br, 4H, $-CH_2-$), 1.41−1.27 (m, 24H, $-CH_2-$ and $-CH_3$), 0.95−0.87 (m, 12H, $-CH_3$). ^{13}C NMR (DMSO-d_6/$CDCl_3$ = 5/1, 75 MHz) δ (ppm): 164.4, 158.3, 158.2, 155.1, 151.9, 146.8, 146.6, 143.0, 140.7, 138.9, 137.5, 137.2, 136.4, 131.9, 131.8, 130.7, 130.6, 129.9, 129.4, 129.3, 129.2, 129.1, 128.8, 128.4, 127.8, 127.4, 126.0, 124.2, 124.1, 123.9, 123.3, 122.9, 122.8, 122.7, 122.4, 121.6, 116.3, 67.6, 31.3, 31.1, 31.0, 30.9, 30.8, 30.4, 29.4, 28.9, 28.8, 28.5, 28.3, 25.3, 22.1, 22.0, 13.6. HRMS (ESI, m/z): $[M-1]^-$ calcd for $C_{80}H_{83}N_2O_4S_2$: 1199.5794. Found: 1199.5802. Anal. calcd for $C_{80}H_{84}N_2O_4S_2$: C, 79.96; H, 7.05; N, 2.33. Found: C, 80.02; H, 7.10; N, 2.17.

Synthesis of ***LI-61***. **LI-61** was synthesized by the similar procedure as **LI-58** described above as a dark red solid (80 mg, 63.5%). ^{1}H NMR ($CDCl_3$, 300 MHz) ($CDCl_3$) δ (ppm): 8.41 (s, 1H, =CH), 8.11 (s, 1H, ArH), 7.92 (s, 1H, ArH), 7.77 (d, J = 8.7 Hz, 2H, ArH), 7.64−7.55 (m, 2H, ArH), 7.44−7.38 (m, 5H, ArH), 7.20−7.15 (m, 7H, ArH), 7.08 (d, J = 9.0 Hz, 4H, ArH), 6.92 (d, J = 8.4 Hz, 2H, ArH), 6.84 (d, J = 8.4 Hz, 4H, ArH), 4.16 (s, br, 4H, $-OCHH_2-$), 3.94 (t, J = 6.6 Hz, 4H, $-OCHH_2-$), 2.81 (s, br, 2H, $-CH_2-$), 2.62 (s, br, 2H, $-CH_2-$), 1.94−1.91 (m, 6H, $-CH_2-$), 1.81−1.75 (m, 6H, $-CH_2-$), 1.60 (s, br, 8H, $-CH_2-$), 1.42−1.27 (m, 28H, $-CH_3$), 0.95−0.87 (m, 18H, $-CH_3$). ^{13}C NMR (DMSO-d_6/$CDCl_3$ = 5/1, 75 MHz) δ (ppm): 164.5, 158.4, 158.2, 155.2, 152.1, 147. 7, 143.1, 140.4, 139.7, 138.6, 138.1, 137.3, 136.4, 132.0, 131.9, 130.9, 130.7, 130.0, 129.5, 129.4, 129.2, 129.0, 128.5, 127.8, 127.4, 126.4, 126.0, 125.6, 125.2, 124.3, 123.4, 122.9, 121.6, 119.0, 116.4, 114.8, 114.1, 96.6, 67.7, 31.2, 31.1, 31.0, 30.9, 29.2, 28.9, 28.8, 28.7, 28.6, 28.5, 25.4, 25.3, 22.1, 13.7. HRMS (ESI, m/z): $[M-1]^-$ calcd for $C_{92}H_{107}N_2O_6S_2$: 1399.7571. Found: 1399.7571. Anal. calcd for $C_{92}H_{108}N_2O_6S_2$: C, 78.82; H, 7.76; N, 2.00. Found: C, 78.95; H, 7.65; N, 1.89.

Device Fabrication and Characterization. Device fabrication and characterization were similar to the reported literature.[52]

RESULTS AND DISCUSSION

Synthesis. The synthetic route to the sensitizers was depicted in Scheme 1. The 9,10-diaryl-substituted anthracene was prepared through two steps. First, 2,6-dibromoanthraquinone reacted with a lithium salt from 1-bromo-4-(*tert*-butyl)benzene or 1-bromo-4-(hexyloxy)benzene, followed by reduction with KI and $NaH_2PO_2{\cdot}H_2O$ to afford **2a** and **2b** in considerable yields. After the Stille coupling reaction with tributyl(4-hexylthiophen-2-yl)stannane, the conjugated bridges of 9,10-diaryl-substituted anthracene and hexylthiophene units were formed. The subsequent Vilsmeier reaction yielded the aldehyde intermediates, which were then converted to the aldehyde precursors through bromination and Suzuki coupling reactions. Finally, the sensitizers were prepared from the aldehydes and cyanoacetic acid in the presence of piperidine, through a Knoevenagel condensation reaction. The sensitizers were characterized by ^{1}H NMR, ^{13}C NMR, mass spectrometry, and elemental analysis.

Optical Properties. Absorption spectra of the sensitizers in a diluted solution of $CHCl_3$ are shown in Figure 1 with their absorption data listed in Table 1. All these sensitizers exhibited three major absorption bands in the range of 300−600 nm. The absorption bands below 420 nm were ascribed to the $\pi-\pi^*$ transition of localized aromatic rings, while the bands in the longer wavelength region (420−600 nm) were derived from ICT. With the introduction of various flexible chains in different positions of the four dyes, their absorption maxima and intensity varied in some degree. The hexyloxy chains,

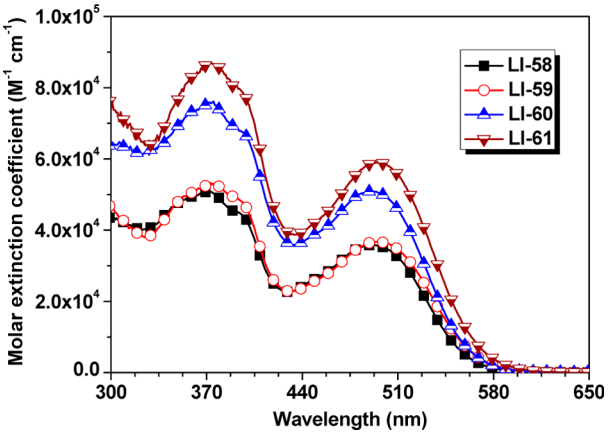

Figure 1. UV−vis spectra of sensitizers in $CHCl_3$.

linked on the donor part, can strengthen the electron-donating ability of triphenylamine unit, leading to a little red-shift (about 5 nm) of the absorption spectra. However, the same chains, bonded on the 9,10-diphenylanthracene group, had little effect on the λ_{max} values of dyes. This was reasonable. 4-Hexyloxyphenyl moieties at the 9 and 10 positions of anthracene were almost perpendicular to the anthracene plane, resulting in the very weak conjugation effect between them. Thus, this kind of hexyloxy group, could not affect the ICT effect apparently, as further confirmed by the theoretical approach. However, the molar extinction coefficients could be sorted by the different groups linked to the 9,10-diphenylanthracene. In this series of dyes, the hexyloxy chains resulted in a stronger absorption than the *tert*-butyl unit, favoring light harvesting.

The absorption spectra of the dyes adsorbed on TiO_2 exhibited broad absorption bands (Figure S1, Supporting Information), which extended beyond 620 nm, and their maximum absorption peaks blue-shifted slightly (about 12−14 nm) in comparison with those in solution. Similar phenomenon has also been reported in the literatures.[48] These blue-shifts may be caused by the dye aggregates or the interaction between dyes and the TiO_2 surface. Actually, the minor shifts would not be liable to form severe dye aggregations on the TiO_2 film. In order to confirm this, we investigated the influence of the co-adsorption of CDCA with different concentrations on the absorption spectra of the dye-adsorbed TiO_2 films (Figure S1, Supporting Information). After the addition of CDCA, the λ_{max} values of the four dyes did not show much change, indicating that these dyes did not form severe aggregation on the surface of TiO_2 but anchored monolayer dyes and contributed to higher solar energy conversion efficiencies of the DSCs.

Electrochemical Properties. To evaluate the possibility of electron transfer from the excited dye to the conduction band of TiO_2, cyclic voltammograms (CV) were performed in CH_2Cl_2 solution with 0.1 M $(n\text{-}C_4H_9)_4NPF_6$ as the electrolyte (Figure 2), and the relevant data were summarized in Table 1.

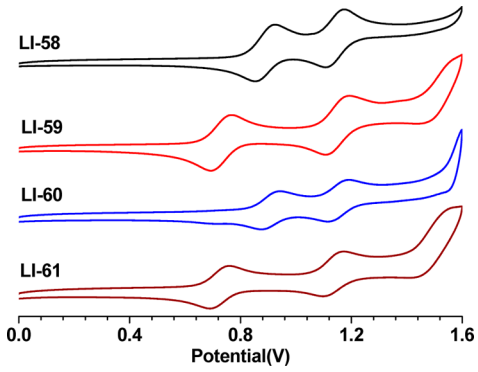

Figure 2. Cyclic voltammograms of sensitizers in CH_2Cl_2.

All the dyes exhibited two quasi-reversible oxidation waves. The first oxidation wave at lower oxidation potential was attributed to the donor, whereas the other at higher oxidation potential was from the spacer. When the hexyloxy chains were linked to the TPA group, the oxidation of **LI-59** and **LI-61** shifted to the lower potentials, compared to those of **LI-58** and **LI-60** with single TPA as the donor group, because the electron excessive hexyloxy chains could strengthen the electron-donating ability of TPA. The oxidation potentials (0.85−1.04 V vs NHE), which were related to their highest occupied molecular orbital (HOMO), were sufficiently more positive than the redox potential of the iodine redox potential (~0.4 V vs NHE) for efficient dye regeneration. Their lowest unoccupied molecular orbital (LUMO) levels of the sensitizers, which were calculated from $E_{ox} - E_{0-0}$, were more negative than the conduction band of TiO_2 (−0.5 V vs NHE), and the overpotentials were in the region of 0.72−0.90 V, providing enough driving force for electron injection.

Theoretical Approach. To gain insight into the geometrical and electronic properties of these sensitizers, the geometries of the dyes have been optimized by using DFT calculations with the Gaussian 09 program.[53] The structures of the dyes were analyzed using a B3LYP/6-31G* hybrid functional for full geometrical optimization. In the ground state, the D−π−A system of these sensitizers had a planar geometry (Figure S2, Supporting Information), especially for the small dihedral angle (~20°) between anthracene and adjacent segments, proving that the 2,6-linked anthracene as

Table 1. Absorbance and Electrochemical Properties of Sensitizers

sensitizer	λ_{abs}[a] ($\varepsilon \times 10^4$ M^{-1} cm^{-1}) (nm)	λ_{max}[b] (nm)	E_{0-0}[c] (eV)	E_{ox}[d] (V) vs NHE	E_{red}[e] (V) vs NHE	E_{gap}[f] (V)
LI-58	372 (5.10), 490 (3.58)	502	2.25	1.00	−1.25	0.75
LI-59	373 (5.33), 495 (3.67)	509	2.25	0.85	−1.40	0.90
LI-60	372 (7.59), 490 (5.10)	502	2.26	1.04	−1.22	0.72
LI-61	373 (8.71), 494 (5.89)	511	2.24	0.85	−1.39	0.89

[a]Absorption spectra of sensitizers measured in $CHCl_3$ with the concentration of 3×10^{-5} mol L^{-1}. [b]Absorption spectra of sensitizers adsorbed on the TiO_2 surface. [c]Bandgap, E_{0-0} was derived from the intersection of absorption and emission spectra. [d]E_{ox} was measured in CH_2Cl_2 with 0.1 M $(n\text{-}C_4H_9)_4NPF_6$ as the electrolyte (scanning rate, 100 mV s^{-1}; working electrode and counter electrode, Pt wires; reference electrode, Ag/AgCl). Oxidation potential (E_{ox}) referenced to calibrated Ag/AgCl was converted to the NHE reference scale: $E_{ox} = E_{ox}^{on} + 0.2$ V. [e]E_{red} was calculated from $E_{ox} - E_{0-0}$. [f]E_{gap} is the energy gap between the E_{red} of dyes and the conduction band level of TiO_2 (−0.5 V vs NHE).

dx.doi.org/10.1021/sc500234a | ACS Sustainable Chem. Eng. 2014, 2, 1776−1784

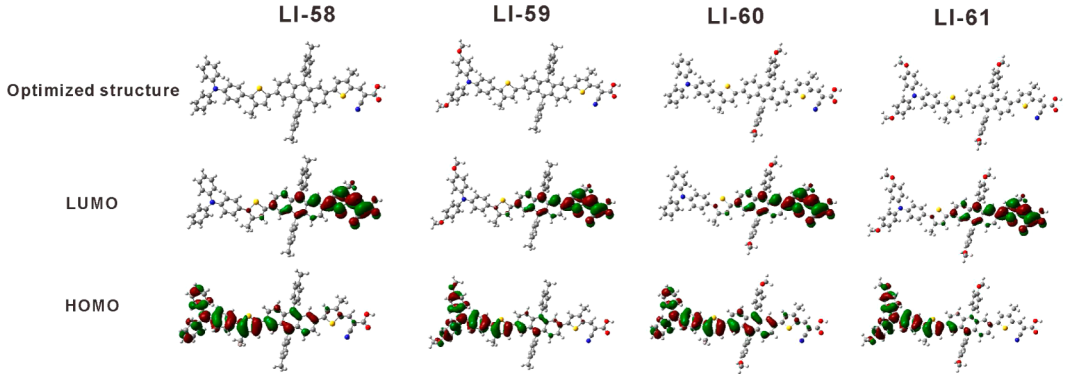

Figure 3. Frontier orbitals of the sensitizers optimized at the B3LYP/6-31G* level.

the conjugated bridge offered a good conjugation from the donor to acceptor. The geometry of 9,10-diarylsubstitued anthracene moieties also matched our idea. 4-*tert*-Butylphenyl or 4-hexyloxyphenyl groups at the 9 and 10 positions of anthracene were almostly perpendicular to the conjugation plane, which could efficiently suppress the possible intermolecular $\pi-\pi$ interactions. Thus, this configuration would not only keep the charge transfer effectively through the whole conjugation system but also suppress the possible $\pi-\pi$ stacking between the sensitizers. The electron distributions of HOMO and LUMO for these sensitizers are shown in Figure 3. HOMO was mainly localized on the triphenylamine and the adjacent thiophene units, and LUMO was localized on the acceptor and adjacent thiophene unit but concentrated on the former. Thus, the HOMO and LUMO were separated, which would lead to efficient intramolecular charge separation with an effective photocurrent generation, finally contributing to improved conversion efficiency.

Photovoltaic Performance of DSCs. The photovoltaic characteristics of these sensitizers were obtained with a sandwich cell using a mixed solvent of acetonitrile and 3-methoxypropionitrile (7:3, v/v) comprising 0.1 M lithium iodide, 0.6 M butylmethylimidazolium iodide (BMII), 0.05 M I_2, and 0.5 M 4-*tert*-butylpyridine (4-TBP) as the redox electrolyte. The action spectra of incident photo-to-current conversion efficiency (IPCE) based on the sensitizers are plotted in Figure 4. It is noted that all the sensitizers showed broad IPCEs in the range of 320−700 nm, in consistent with the electronic absorption spectra of dye-coated TiO_2 films. All

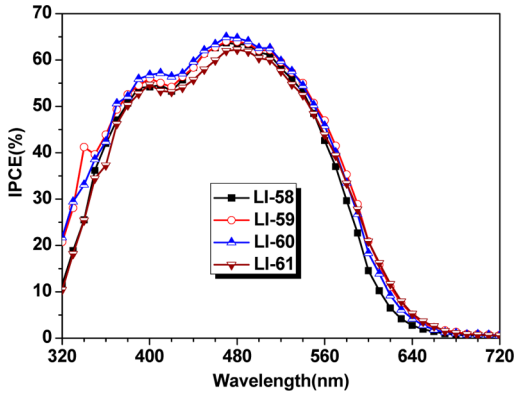

Figure 4. Spectra of monochromatic incident photon-to-current conversion efficiency (IPCE) for DSCs based on the sensitizers.

the dyes showed similar IPCE values, and the values exceeded 50% from 380 to 560 nm.

Figure 5 showed the current−voltage characteristics of DSCs fabricated with these sensitizers under standard global AM 1.5

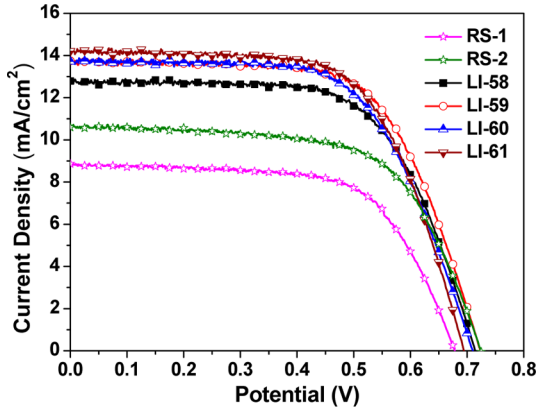

Figure 5. $J-V$ characteristics of DSCs measured at simulated 100 mW cm^{-2} AM1.5 conditions.

solar light conditions. The photovoltaic characteristic parameters of short-circuit current density (J_{sc}), open-circuit voltage (V_{oc}), fill factor (FF), and photovoltaic conversion efficiency (η) are summarized in Table 2 and Figure S3 of the Supporting Information. In order to highlight the function of anthracene, the photovoltaic performances of anthrancene-based dyes and references were tested under similar conditions, and the corresponding data were presented in Table 1 and Table S1 of the Supporting Information. Compared to the reference sensitizers, the anthracene dyes showed improved J_{sc} values and conversion efficiencies. For example, the **RS-1** sensitized solar cell exhibited a J_{sc} of 8.77 mA cm^{-2}, V_{oc} of 684 mV, and FF of 0.65, corresponding to a η value of 3.93%. Once the anthrancene derivatives were incorporated into the conjugated bridge to form the dyes of **LI-58** and **LI-59**, the J_{sc} values increased to 12.24 and 13.68 mA cm^{-2}, respectively. Accordingly, the conversion efficiencies were enhanced about 50%. These results suggested that the addition of anthracene derivatives can strengthen the light-harvesting abilities and suppress the possible dye aggregates, which were beneficial to achieving better photovoltaic performance. The DSC sensitized with **LI-58**, bearing triphenylamine as the donor and 9,10-di-4-*tert*-butylphenyl anthracene as the conjugated bridge, showed a J_{sc} of 12.24 mA cm^{-2}, V_{oc} of 707 mV, and FF of 0.65, corresponding to a η value of 5.59%. Under the same

dx.doi.org/10.1021/sc500234a | ACS Sustainable Chem. Eng. 2014, 2, 1776−1784

Table 2. Performance Data of Dye Sensitized Solar Cells

sensitizer	J_{sc} (mA cm^{-2})	V_{oc} (mV)	FF	η (%)	R_{rec} (ohm)	τ_n (ms)
RS-1	8.77 ± 0.22	684 ± 8	0.65 ± 0.01	3.93 ± 0.18		
RS-2	10.59 ± 0.20	727 ± 3	0.66 ± 0.01	5.06 ± 0.14		
LI-58	12.24 ± 0.48	707 ± 11	0.65 ± 0.01	5.59 ± 0.24	76.61	23.90
LI-59	13.42 ± 0.22	722 ± 1	0.66 ± 0.01	6.42 ± 0.04	91.86	24.76
LI-60	13.68 ± 0.23	708 ± 12	0.63 ± 0.02	6.10 ± 0.20	71.96	19.51
LI-61	14.20 ± 0.47	699 ± 8	0.63 ± 0.02	6.29 ± 0.10	53.96	13.49
N719	17.00 ± 0.07	717 ± 14	0.62 ± 0.02	7.52 ± 0.19		

conditions, the photovoltaic characteristics of **LI-59** with a stronger donor of hexyloxy-substituted triphenylamine, including J_{sc}, V_{oc}, FF, and η, were 13.42 mA cm^{-2}, 722 mV, 0.66, and 6.42%, respectively. These better results were reasonable. First, the electron-donating alkoxy groups attached on the donor could elevate the HOMO level of **LI-59**, resulting in a broader absorption spectra than that of **LI-58**, which could consequently contribute to an increased J_{sc}. Besides, the introduced alkoxy groups might aid to suppress the charge recombination between the injected electrons and eletrolyte, thus giving a higher V_{oc}. In addition to the hexyloxy-substituted triphenylamine, the different peripheral-substituted groups in the 9 and 10 positions of anthracene could also play an important role for high performance of the solar cells. As mentioned above, these aromatic groups, with large dihedral angles against the anthracene moieties, could help suppress the harmful $\pi-\pi$ stacking and dye aggregations on the thin film of TiO_2. Also, these substituted aromatic rings could be further modified on the molecular level. When keeping triphenylamine as the electron donor, the substituted groups at the 9 and 10 positions could be changed from 4-*tert*-butylphenyl to 4-hexyloxyphenyl, and the resultant dye of **LI-60** displayed an increased J_{sc} of 13.68 mA cm^{-2} compared to that of **LI-58** (12.24 mA cm^{-2}), leading to a progressive conversion efficiency of 6.10%. Further replacing the triphenylamine with hexyloxy-substituted triphenylamine as the donor one, in the case of **LI-61**, the J_{sc} value could be increased to 14.20 mA cm^{-2}, with a conversion efficiency of 6.29%. Keeping the conjugated skeleton as the same, the relatively higher J_{sc} values of **LI-60** and **LI-61** indicated that the better light-harvesting abilities should be partly derived from the substituted moieties to the anthracene unit.

Chenodeoxycholic acid (CDCA) is a nonchromophoric coadsorbent, which was usually co-deposited onto the surface of TiO_2 films to displace dye molecules and hinder the formation of dye aggregates, and generally, it could lead to an improved J_{sc}. Actually, some organic dyes featuring fuse rings, once co-deposited with CDCA, exhibited much improved photovoltaic conversion efficiencies, disclosing that the dye sensitizers with good planar structures would easily form the severe dye aggregates on the TiO_2 surface. In our case, the photovoltaic properties of the DSCs with various concentrations of CDCA were studied in detail. Before dipping into the $CHCl_3$ solution of dyes, TiO_2 films were pretreated with different concentrations of CDCA in ethanol solution for 6 h, as presented in Table S1 and Figure S4 of the Supporting Information. Interestingly, even when a low concentration of CDCA was applied, all of the J_{sc} and η values did not increase in comparison with those of the devices without CDCA, partially indicating that the sensitizers bearing 9,10-diaryl-substituted anthracene did not form severe aggregates on the surface of TiO_2 films. On the contrary, the addition of CDCA reduced the dye density on the TiO_2 surface, causing possibly decreased conversion efficiencies. This, perhaps, on another side, further confirmed the important role of the aromatic rings in 9 and 10 positions of anthracene moieties. Thus, the unwanted $\pi-\pi$ stacking of the 2,6-conjugated anthracene dyes could be partially resolved by the introduction of some aromatic groups at the 9 and 10 positions of the anthracene ring. By further optimizing the structure of anthracene-based dye, especially by fully utilizing the four functional sites of the authracene core, new dyes with better performance might be achieved.

Electrochemical Impedance Spectroscopy. Electrochemical impedance spectroscopy (EIS) was measured in the dark under a forward bias of −0.70 V with a frequency range of 0.1 Hz to 100 kHz to elucidate the correlation of V_{oc} with the dyes. Figure 6 showed both the Nyquist plots and Bode phase plots of the DSCs based on dyes **LI-58** and **LI-61**. In the Nyquist plot, the larger semcircle at the intermediated frequency reflected the charge transfer resistance at the TiO_2/dye/electrolyte interface. The charge recombination resistance at the TiO_2 surface, R_{rec}, could be deduced by fitting the curves using a Z-view software, as presented in Table 2. The increased R_{rec} values implied the retardation of charge

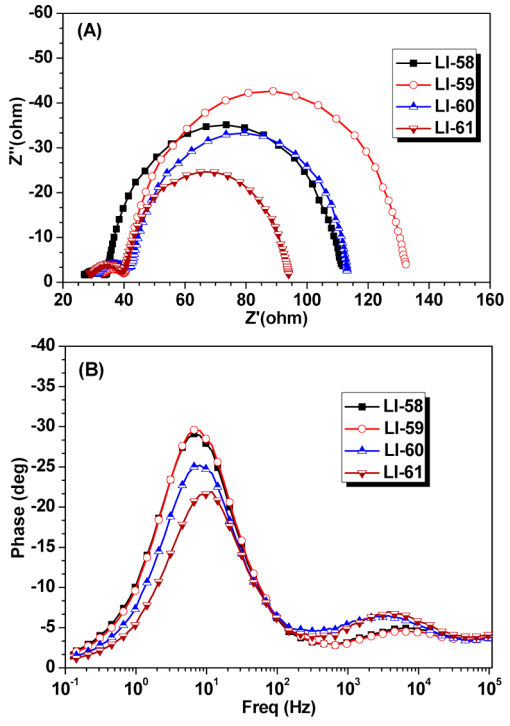

Figure 6. Electrochemical impedance spectroscopy (EIS) for DSCs based on the sensitizers. (A) Nyquist plots in the dark. (B) Bode phase plots in the dark.

dx.doi.org/10.1021/sc500234a | ACS Sustainable Chem. Eng. 2014, 2, 1776−1784

recombination between the injected electron in the TiO_2 and oxidized species in the electrolyte; in other words, the larger R_{rec} meant a slower charge recombination rate. The charge recombination rate decreased in the order of **LI-61** > **LI-60** ≈ **LI-58** > **LI-59**, which was in accordance with the trend of V_{oc}. These results suggested that the charge recombination rate could be partially suppressed by the introduction of alkyl or alkoxy chains, and the flexible chains in different positions of the dyes could play the different roles. The main role of the alkoxy group in the donor part was to form the blocking layer, with the aim to prevent the oxidized species from contacting with the injected electron in the TiO_2. However, the flexible chains in the π bridge primarily act as the isolation group to suppress the possible $\pi-\pi$ stacking, which was beneficial to the arrangements of the dyes on the TiO_2 film. **LI-59** showed the largest R_{rec} value, possibly due to the combined action of the hexyloxy chain in the donor part and the *t*-butyl moieties as the isolation group, which could form the blocking layer and keep the compact layer of dyes on the TiO_2 surface.

The characteristic frequency in the Bode plot was related to the charge recombination rate, and its reciprocal was associated with the electron lifetime. Correspondingly, the characteristic frequency peaks in the Bode phase plots (Figure 6B) decreased in the order of **LI-61** > **LI-60** > **LI-58** > **LI-59**, and the electron lifetime was enhanced in reverse with the calculated values of 13.49, 19.51, 23.90, and 24.76 ms, respectively. Thus, **LI-59** had the longest electron lifetime, suggesting a more effective suppression of the back reaction, which would result in improved V_{oc}.

CONCLUSION

In summary, 9,10-diaryl-substituted anthracene moieties have been introduced into organic dyes as the conjugated bridge. Because the bulky substituted groups in the C9 and C10 positions were almost perpendicular to the conjugated system, these anthracene-based dyes were not liable to form severe dye aggregates on the TiO_2 surface, which was beneficial to increasing the efficiency of electron injection and suppressing the possible electron recombination arising from electrons in the TiO_2 film and electrolyte, leading to enhancement of conversion efficiency. Additionally, with different flexible chains linked to the 9,10-diaryl-substituted anthracene unit, the photovoltaic performance of these dyes could be optimized in some degree. These results indicated that molecular engineering is crucial for the construction of high conversion efficiency solar cells, and the 9,10-diaryl-substituted anthracene-based dyes might be a good choice for the design of high-efficiency organic sensitizers.

ASSOCIATED CONTENT

Supporting Information

Synthesis of the intermediates, figures of UV−vis spectra on TiO_2 film, optimized structures of the sensitizers, *J*−*V* characteristics of DSCs with different concentrations of CDCA, and photovoltaic performance parameters. This material is available free of charge via the Internet at http://pubs.acs.org.

AUTHOR INFORMATION

Corresponding Author

*Phone: +86-27-68755363. Fax: +86-27-68755363. E-mail: qianqian-alinda@163.com.

Notes

The authors declare no competing financial interest.

ACKNOWLEDGMENTS

We are grateful to the National Science Foundation of China (21372003) and National Fundamental Key Research Program (2013CB834701) for financial support.

REFERENCES

(1) O'Regan, B.; Gratzel, M. A low-cost, high-efficiency solar cell based on dye-sensitized colloidal TiO_2 films. *Nature* **1991**, *353*, 737−740.

(2) Yella, A.; Lee, H.-W.; Tsao, H. N.; Yi, C.; Chandiran, A. K.; Nazeeruddin, M. K.; Diau, E. W.-G.; Yeh, C.-Y.; Zakeeruddin, S. M.; Grätzel, M. Porphyrin-sensitized solar cells with cobalt (II/III)-based redox electrolyte exceed 12% efficiency. *Science* **2011**, *334*, 629−634.

(3) Zhang, S.; Yang, X.; Numata, Y.; Han, L. Highly efficient dye-sensitized solar cells: Progress and future challenges. *Energy Environ. Sci.* **2013**, *6*, 1443−1464.

(4) Wu, Y.; Zhu, W. Organic sensitizers from D-π-A to D-A-π-A: Effect of the internal electron-withdrawing units on molecular absorption, energy levels and photovoltaic performances. *Chem. Soc. Rev.* **2013**, *42*, 2039−2058.

(5) Nazeeruddin, M. K.; De Angelis, F.; Fantacci, S.; Selloni, A.; Viscardi, G.; Liska, P.; Ito, S.; Takeru, B.; Grätzel, M. Combined experimental and DFT-TDDFT computational study of photoelectrochemical cell ruthenium sensitizers. *J. Am. Chem. Soc.* **2005**, *127*, 16835−16847.

(6) Gao, F.; Wang, Y.; Shi, D.; Zhang, J.; Wang, M.; Jing, X.; Humphry-Baker, R.; Wang, P.; Zakeeruddin, S. M.; Grätzel, M. Enhance the optical absorptivity of nanocrystalline T iO_2 film with high molar extinction coefficient ruthenium sensitizers for high performance dye-sensitized solar cells. *J. Am. Chem. Soc.* **2008**, *130*, 10720−10728.

(7) Chang, Y.-C.; Wang, C.-L.; Pan, T.-Y.; Hong, S.-H.; Lan, C.-M.; Kuo, H.-H.; Lo, C.-F.; Hsu, H.-Y.; Lin, C.-Y.; Diau, E. W.-G. A strategy to design highly efficient porphyrin sensitizers for dye-sensitized solar cells. *Chem. Commun.* **2011**, *47*, 8910−8912.

(8) Li, L.-L.; Diau, E. W.-G. Porphyrin-sensitized solar cells. *Chem. Soc. Rev.* **2013**, *42*, 291−304.

(9) Wang, C.-L.; Lan, C.-M.; Hong, S.-H.; Wang, Y.-F.; Pan, T.-Y.; Chang, C.-W.; Kuo, H.-H.; Kuo, M.-Y.; Diau, E. W.-G.; Lin, C.-Y. Enveloping porphyrins for efficient dye-sensitized solar cells. *Energy Environ. Sci.* **2012**, *5*, 6933−6940.

(10) Yella, A.; Humphry-Baker, R.; Curchod, B. F. E.; Ashari Astani, N.; Teuscher, J.; Polander, L. E.; Mathew, S.; Moser, J.-E.; Tavernelli, I.; Rothlisberger, U.; Grätzel, M.; Nazeeruddin, M. K.; Frey, J. Molecular engineering of a fluorene donor for dye-sensitized solar cells. *Chem. Mater.* **2013**, *25*, 2733−2739.

(11) Ren, X.; Jiang, S.; Cha, M.; Zhou, G.; Wang, Z.-S. Thiophene-bridged double D-π-A dye for efficient dye-sensitized solar cell. *Chem. Mater.* **2012**, *24*, 3493−3499.

(12) Zeng, W.; Cao, Y.; Bai, Y.; Wang, Y.; Shi, Y.; Zhang, M.; Wang, F.; Pan, C.; Wang, P. Efficient dye-sensitized solar cells with an organic photosensitizer featuring orderly conjugated ethylenedioxythiophene and dithienosilole blocks. *Chem. Mater.* **2010**, *22*, 1915−1925.

(13) Li, Q.; Lu, L.; Zhong, C.; Huang, J.; Huang, Q.; Shi, J.; Jin, X.; Peng, T.; Qin, J.; Li, Z. New pyrrole-based organic dyes for dye-sensitized solar cells: Convenient syntheses and high efficiency. *Chem.-Eur. J.* **2009**, *15*, 9664−9668.

(14) Liang, M.; Chen, J. Arylamine organic dyes for dye-sensitized solar cells. *Chem. Soc. Rev.* **2013**, *42*, 3453−3488.

(15) Hao, X.; Liang, M.; Cheng, X.; Pian, X.; Sun, Z.; Xue, S. Organic dyes incorporating the benzo[1,2-b:4,5-b′]dithiophene moiety for efficient dye-sensitized solar cells. *Org. Lett.* **2011**, *13*, 5424−5427.

(16) Lim, K.; Ju, M. J.; Na, J.; Choi, H.; Song, M. Y.; Kim, B.; Song, K.; Yu, J.-S.; Kim, E.; Ko, J. Molecular engineering of organic

sensitizers with planar bridging units for efficient dye-sensitized solar cells. *Chem. -Eur. J.* **2013**, *19*, 9442−9446.
(17) Zhu, X.; Tsuji, H.; Yella, A.; Chauvin, A.-S.; Gratzel, M.; Nakamura, E. New sensitizers for dye-sensitized solar cells featuring a carbon-bridged phenylenevinylene. *Chem. Commun.* **2013**, *49*, 582−584.
(18) Lu, X.; Zhou, G.; Wang, H.; Feng, Q.; Wang, Z.-S. Near infrared thieno[3,4-b]pyrazine sensitizers for efficient quasi-solid-state dye-sensitized solar cells. *Phys. Chem. Chem. Phys.* **2012**, *14*, 4802−4809.
(19) Yao, Z.; Yang, L.; Cai, Y.; Yan, C.; Zhang, M.; Cai, N.; Dong, X.; Wang, P. Rigidifying the π-linker to enhance light absorption of organic dye-sensitized solar cells and influences on charge transfer dynamics. *J. Phys. Chem. C* **2014**, *118*, 2977−2986.
(20) Zhang, G.; Bala, H.; Cheng, Y.; Shi, D.; Lv, X.; Yu, Q.; Wang, P. High efficiency and stable dye-sensitized solar cells with an organic chromophore featuring a binary π-conjugated spacer. *Chem. Commun.* **2009**, *45*, 2198−2200.
(21) Xu, M.; Zhou, D.; Cai, N.; Liu, J.; Li, R.; Wang, P. Electrical and photophysical analyses on the impacts of arylamine electron donors in cyclopentadithiophene dye-sensitized solar cells. *Energy Environ. Sci.* **2011**, *4*, 4735−4742.
(22) Cao, Y.; Cai, N.; Wang, Y.; Li, R.; Yuan, Y.; Wang, P. Modulating the assembly of organic dye molecules on titania nanocrystals via alkyl chain elongation for efficient mesoscopic cobalt solar cells. *Phys. Chem. Chem. Phys.* **2012**, *14*, 8282−8286.
(23) Jiang, S.; Lu, X.; Zhou, G.; Wang, Z.-S. Charge transfer in cross conjugated 4,8-dithienylbenzo[1,2-b:4,5-b′]dithiophene based organic sensitizers. *Chem. Commun.* **2013**, *49*, 3899−3901.
(24) Yang, J.; Guo, F.; Hua, J.; Li, X.; Wu, W.; Qu, Y.; Tian, H. Efficient and stable organic DSSC sensitizers bearing quinacridone and furan moieties as a planar π-spacer. *J. Mater. Chem.* **2012**, *22*, 24356−24365.
(25) Kanaparthi, R. K.; Kandhadi, J.; Giribabu, L. Metal-free organic dyes for dye-sensitized solar cells: recent advances. *Tetrahedron* **2012**, *68*, 8383−8393.
(26) Hagfeldt, A.; Boschloo, G.; Sun, L.; Kloo, L.; Pettersson, H. Dye-sensitized solar cells. *Chem. Rev.* **2010**, *110*, 6595−6663.
(27) Cui, W.; Wu, Y.; Tian, H.; Geng, Y.; Wang, F. The first soluble conjugated poly(2,6-anthrylene): synthesis and properties. *Chem. Commun.* **2008**, *44*, 1017−1019.
(28) Chun, D.; Cheng, Y.; Wudl, F. The most stable and fully characterized functionalized heptacene. *Angew. Chem., Int. Ed.* **2008**, *47*, 8380−8385.
(29) Park, J.-H.; Chung, D. S.; Park, J.-W.; Ahn, T.; Kong, H.; Jung, Y. K.; Lee, J.; Yi, M. H.; Park, C. E.; Kwon, S.-K.; Shim, H.-K. Soluble and easily crystallized anthracene derivatives: Precursors of solution-processable semiconducting molecules. *Org. Lett.* **2007**, *9*, 2573−2576.
(30) Chen, H.-Y.; Chen, C.-T.; Chen, C.-T. Synthesis and characterization of a new series of blue fluorescent 2,6-linked 9,10-diphenylanthrylenephenylene copolymers and their application for polymer light-emitting diodes. *Macromolecules* **2010**, *43*, 3613−3623.
(31) Wu, C.-H.; Chien, C.-H.; Hsu, F.-M.; Shih, P.-I.; Shu, C.-F. Efficient non-doped blue-light-emitting diodes incorporating an anthracene derivative end-capped with fluorene groups. *J. Mater. Chem.* **2009**, *19*, 1464−1470.
(32) Chien, C.-H.; Chen, C.-K.; Hsu, F.-M.; Shu, C.-F.; Chou, P.-T.; Lai, C.-H. Multifunctional deep-blue emitter comprising an anthracene core and terminal triphenylphosphine oxide groups. *Adv. Funct. Mater.* **2009**, *19*, 560−566.
(33) Kim, Y. H.; Jeong, H. C.; Kim, S. H.; Yang, K.; Kwon, S. K. High-purity-blue and high-efficiency electroluminescent devices based on anthracene. *Adv. Funct. Mater.* **2005**, *15*, 1799−1805.
(34) Jung, K. H.; Bae, S. Y.; Kim, K. H.; Cho, M. J.; Lee, K.; Kim, Z. H.; Choi, D. H.; Lee, D. H.; Chung, D. S.; Park, C. E. High-mobility anthracene-based X-shaped conjugated molecules for thin film transistors. *Chem. Commun.* **2009**, *45*, 5290−5292.
(35) Park, J.-H.; Lee, D. H.; Kong, H.; Park, M.-J.; Jung, I. H.; Park, C. E.; Shim, H.-K. Organic thin-film transistor properties and the structural relationships between various aromatic end-capped triisopropylsilylethynyl anthracene derivatives. *Org. Electron.* **2010**, *11*, 820−830.
(36) Egbe, D. A. M.; Türk, S.; Rathgeber, S.; Kühnlenz, F.; Jadhav, R.; Wild, A.; Birckner, E.; Adam, G.; Pivrikas, A.; Cimrova, V.; Knör, G. n.; Sariciftci, N. S.; Hoppe, H. Anthracene based conjugated polymers: Correlation between π-π-stacking ability, photophysical properties, charge carrier mobility, and photovoltaic performance. *Macromolecules* **2010**, *43*, 1261−1269.
(37) Rathgeber, S.; Bastos de Toledo, D.; Birckner, E.; Hoppe, H.; Egbe, D. A. M. Intercorrelation between structural ordering and emission properties in photoconducting polymers. *Macromolecules* **2009**, *43*, 306−315.
(38) Teng, C.; Yang, X.; Yang, C.; Li, S.; Cheng, M.; Hagfeldt, A.; Sun, L. Molecular design of anthracene-bridged metal-free organic dyes for efficient dye-sensitized solar cells. *J. Phys. Chem. C* **2010**, *114*, 9101−9110.
(39) Lin, Y.-Z.; Huang, C. H.; Chang, Y. J.; Yeh, C.-W.; Chin, T.-M.; Chi, K.-M.; Chou, P.-T.; Watanabe, M.; Chow, T. J. Anthracene based organic dipolar compounds for sensitized solar cells. *Tetrahedron* **2014**, *70*, 262−269.
(40) Rathgeber, S.; Perlich, J.; Kühnlenz, F.; Türk, S.; Egbe, D. A. M.; Hoppe, H.; Gehrke, R. Correlation between polymer architecture, mesoscale structure and photovoltaic performance in side-chain-modified poly(p-arylene-ethynylene)-alt-poly(p-arylene-vinylene): PCBM bulk-heterojunction solar cells. *Polymer* **2011**, *52*, 3819−3826.
(41) Justin Thomas, K. R.; Singh, P.; Baheti, A.; Hsu, Y.-C.; Ho, K.-C.; Lin, J. T. Electro-optical properties of new anthracene based organic dyes for dye-sensitized solar cells. *Dye Pigm.* **2011**, *91*, 33−43.
(42) Yeh-Yung Lin, R.; Lin, H.-W.; Yen, Y.-S.; Chang, C.-H.; Chou, H.-H.; Chen, P.-W.; Hsu, C.-Y.; Chen, Y.-C.; Lin, J. T.; Ho, K.-C. 2,6-Conjugated anthracene sensitizers for high-performance dye-sensitized solar cells. *Energy Environ. Sci.* **2013**, *6*, 2477−2486.
(43) Almeataq, M. S.; Yi, H.; Al-Faifi, S.; Alghamdi, A. A. B.; Iraqi, A.; Scarratt, N. W.; Wang, T.; Lidzey, D. G. Anthracene-based donor-acceptor low band gap polymers for application in solar cells. *Chem. Commun.* **2013**, *49*, 2252−2254.
(44) Ito, K.; Suzuki, T.; Sakamoto, Y.; Kubota, D.; Inoue, Y.; Sato, F.; Tokito, S. Oligo(2,6-anthrylene)s: Acene-oligomer approach for organic field-effect transistors. *Angew. Chem., Int. Ed.* **2003**, *115*, 1191−1194.
(45) Becker, H. D.; Langer, V.; Sieler, J.; Becker, H. C. Molecular conformations of 9,9′-bianthryl, di-9-anthrylmethane, and some related twisted anthracene derivatives. *J. Org. Chem.* **1992**, *57*, 1883−1887.
(46) Sun, J.; Chen, J.; Zou, J.; Ren, S.; Zhong, H.; Zeng, D.; Du, J.; Xu, E.; Fang, Q. π-Conjugated poly(anthracene-alt-fluorene)s with X-shaped repeating units: New blue-light emitting polymers. *Polymer* **2008**, *49*, 2282−2287.
(47) Buhbut, S.; Clifford, J. N.; Kosa, M.; Anderson, A. Y.; aShalom, M.; Major, D. T.; Palomares, E.; Zaban, A. Controlling dye aggregation, injection energetics and catalytic recombination in organic sensitizer based dye cells using a single electrolyte additive. *Energy Environ. Sci.* **2013**, *6*, 3046−3053.
(48) Pei, K.; Wu, Y.; Islam, A.; Zhang, Q.; Han, L.; Tian, H.; Zhu, W. Constructing high-efficiency D-A-π-A-featured solar cell sensitizers: a promising building block of 2,3-diphenylquinoxaline for anti-aggregation and photostability. *ACS Appl. Mater. Interfaces* **2013**, *5*, 4986−4995.
(49) Chen, J.-H.; Tsai, C.-H.; Wang, S.-A.; Lin, Y.-Y.; Huang, T.-W.; Chiu, S.-F.; Wu, C.-C.; Wong, K.-T. Organic dyes containing a coplanar indacenodithiophene bridge for high-performance dye-sensitized solar cells. *J. Org. Chem.* **2011**, *76*, 8977−8985.
(50) Duan, T.; Fan, K.; Zhong, C.; Chen, X.; Peng, T.; Qin, J. A new class of organic dyes containing β-substituted 2, 2′-bithiophenene unit as a π-linker for dye-sensitized solar cells: Structural modification for understanding relationship of structure and photovoltaic performances. *J. Power Sources* **2013**, *234*, 23−30.
(51) Liu, J.; Zhou, D.; Wang, F.; Fabregat-Santiago, F.; Miralles, S. G.; Jing, X.; Bisquert, J.; Wang, P. Joint photophysical and electrical

analyses on the influence of conjugation order in D-π-A photosensitizers of mesoscopic titania solar cells. *J. Phys. Chem. C* **2011**, *115*, 14425−14430.

(52) Li, H.; Hou, Y.; Yang, Y.; Tang, R.; Chen, J.; Wang, H.; Han, H.; Peng, T.; Li, Q.; Li, Z. Attempt to improve the performance of pyrrole-containing dyes in dye sensitized solar cells by adjusting isolation groups. *ACS Appl. Mater. Interfaces* **2013**, *5*, 12469−12477.

(53) Frisch, M. J.; Trucks, G. W.; Schlegel, H. B.; Scuseria, G. E.; Robb, M. A.; Cheeseman, J. R.; Scalmani, G.; Barone, V.; Mennucci, B.; Petersson, G. A.; Nakatsuji, H.; Caricato, M.; Li, X.; Hratchian, H. P.; Izmaylov, A. F.; Bloino, J.; Zheng, G.; Sonnenberg, J. L.; Hada, M.; Ehara, M.; Toyota, K.; Fukuda, R.; Hasegawa, J.; Ishida, M.; Nakajima, T.; Honda, Y.; Kitao, O.; Nakai, H.; Vreven, T.; Montgomery, Jr., J. A.; Peralta, J. E.; Ogliaro, F.; Bearpark, M.; Heyd, J. J.; Brothers, E.; Kudin, K. N.; Staroverov, V. N.; Kobayashi, R.; Normand, J.; Raghavachari, K.; Rendell, A.; Burant, J. C.; Iyengar, S. S.; Tomasi, J.; Cossi, M.; Rega, N.; Millam, J. M.; Klene, M.; Knox, J. E.; Cross, J. B.; Bakken, V.; Adamo, C.; Jaramillo, J.; Gomperts, R.; Stratmann, R. E.; Yazyev, O.; Austin, A. J.; Cammi, R.; Pomelli, C.; Ochterski, J. W.; Martin, R. L.; Morokuma, K.; Zakrzewski, V. G.; Voth, G. A.; Salvador, P.; Dannenberg, J. J.; Dapprich, S.; Daniels, A. D.; Farkas, Ö.; Foresman, J. B.; Ortiz, J. V.; Cioslowski, J.; Fox, D. J. *Gaussian 09*; Gaussian, Inc., Wallingford, CT, 2009.